Title	Extreme location of F drip line and disappearance of the N=20 magic structure
Author(s)	Yutaka Utsuno, Takaharu Otsuka, Takahiro Mizusaki, and Michio Honma
Citation	Physical Review C, 64(1), 011301 (2001).
Text Version	Publisher
URL	http://jolissrch-inter.tokai-sc.jaea.go.jp/search/servlet/search?12683
DOI	http://dx.doi.org/10.1103/PhysRevC.64.011301
Right	© American Physical Society

PHYSICAL REVIEW C, VOLUME 64, 011301(R)

Extreme location of F drip line and disappearance of the $N=20$ magic structure

Yutaka Utsuno,[1] Takaharu Otsuka,[2,3] Takahiro Mizusaki,[4] and Michio Honma[5]
[1]*Japan Atomic Energy Research Institute, Tokai, Ibaraki 319-1195, Japan*
[2]*Department of Physics, University of Tokyo, Hongo, Bunkyo-ku, Tokyo 113-0033, Japan*
[3]*RIKEN, Hirosawa, Wako-shi, Saitama 351-0198, Japan*
[4]*Department of Law, Senshu University, Higashimita, Tama, Kawasaki, Kanagawa 214-8580, Japan*
[5]*Center for Mathematical Sciences, University of Aizu, Tsuruga, Ikki-machi, Aizu-Wakamatsu, Fukushima 965-8580, Japan*
(Received 14 September 2000; published 4 June 2001)

The drip line of F isotopes is discussed from the viewpoint of a unified description of exotic nuclei with $N\sim20$. The structure of those nuclei is described by means of large-scale shell model calculations, most of which are Monte Carlo shell model. It is shown that, due to the narrowing of the $N=20$ shell gap towards smaller Z, the mixing among normal, intruder, and higher intruder configurations can be enhanced significantly, and can produce crucial effects, including the F drip line located extremely far from the O drip line. The feasibility of Monte Carlo shell model is demonstrated for systems with an odd number of fermions.

DOI: 10.1103/PhysRevC.64.011301 PACS number(s): 21.60.Cs, 21.60.Ka, 27.30.+t

The existence of a given nucleus is one of the most basic questions nuclear physics must answer. A recent puzzling and intriguing problem in this direction is why the drip line of F isotopes is located farther away as compared to that of O isotopes: at least six more neutrons can be contained in F isotopes, whereas there is just one more proton [1,2]. The heaviest observed F isotope is ^{31}F where the neutron number is $N=22$. For such neutron-rich nuclei with $N\sim20$, the disappearance of the $N=20$ magic structure has been studied. Independently of whether it is correct or not, this disappearance can be discussed in reference to the picture of the *island of inversion* [3]: a small region of the nuclear chart where the ground state consists of *intruder* configurations with two neutrons excited from the sd shell to the pf shell, while *normal* states, where no such excitations occur, are lying higher. This inversion is due to the large deformation energy in the intruder configurations as suggested in [4]. The F isotopes are outside this *island* [3], mainly because one valence proton is too few to produce a large deformation energy. Thus, the relation between the drip line of F isotopes located very far and the disappearance of the $N=20$ magic structure is a puzzle. In this Rapid Communication, on the basis of large-scale shell model calculations, we shall suggest a basic mechanism to extend the F drip line, as a consequence of a unified description for exotic nuclei with $N\sim20$, and we shall explain how these two phenomena are linked.

The structure of those exotic nuclei is studied, in this Rapid Communication, by shell-model calculations with unrestricted mixing among relevant particle-hole configurations, so as to incorporate various dynamical effects including those absent in the model of the *island of inversion*. In fact, by doing this kind of calculation, one can see for which states the model appears to be reasonable. Such calculations have, however, remained unfeasible until recently due to the huge dimension of the Hilbert space in which the Hamiltonian matrix is diagonalized, and various truncations were introduced in conventional shell-model calculations [5–7].

The Monte Carlo shell model (MCSM) has recently been proposed and developed, and it is suitable for studying the present issues. The MCSM implies applications of the quantum Monte Carlo diagonalization (QMCD) method [8–11] to the nuclear shell model. In the MCSM calculation, the most important basis vectors of the many-body Hilbert space are selected as characterized by the *importance truncation* (to the exact calculation) [12]. In an earlier report [13], the MCSM was applied to the study of yrast states of O, Ne, Mg, and Si isotopes, demonstrating that the properties of those states can be described quite nicely within a single framework. On the other hand, the boundary of the *island of inversion* turned out to be rather indefinite. For instance, ^{28}Ne is classified as a *normal* nucleus in the *island of inversion* picture, whereas in the calculation of [13] it is just on the boundary, having normal and intruder configurations to nearly the same amounts in its ground state. This structure appeared to be in good agreement with experiments on the first 2^+ level [14] and on its $E2$ strength [15].

The Hamiltonian and the model space are the same as those used in the above-mentioned calculations in [13]. In order to study the structure of F isotopes, however, one has to examine the validity of the Hamiltonian and model space for odd-Z nuclei with $N\sim20$, and, in particular, its capability of handling normal and intruder configurations. For this purpose, we carry out a systematic MCSM calculation of $N=20$ nuclei including ^{29}F, ^{31}Na, and ^{33}Al. We mention that the present work is the first MCSM calculation of odd-A nuclei, and it should confirm the feasibility of MCSM calculation for odd-A nuclei. Odd-A nuclei have been rather difficult objects in usual quantum Monte Carlo methods because of the minus sign problem which is rather severe for even-even nuclei but becomes more severe for odd-A nuclei. For instance, it has been known that, in the shell model Monte Carlo calculations, odd-A nuclei cannot be treated in the same way as even-even nuclei [16]. In the MCSM, there is no sign problem, or no formal difference between even-even and odd-A nuclei. However, since the sign problem occurs so severely for odd-A nuclei in other Monte Carlo approaches, one may suspect that the practical aspect of MCSM might be affected. We therefore should examine whether or not MCSM calculations can be performed in practice for odd-A nuclei with a small number of basis vec-

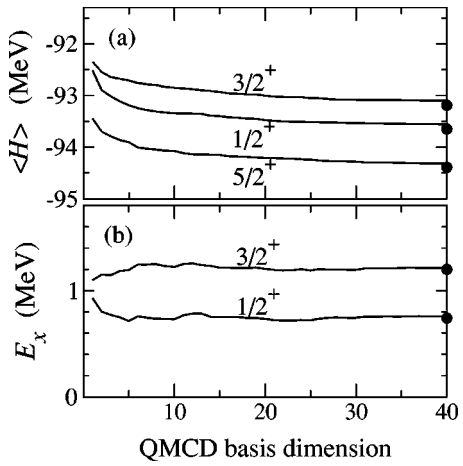

FIG. 1. (a) Total energies and (b) excitation energies of ^{25}Mg calculated by the MCSM as a function of the QMCD basis dimension. Circles denote exact solutions.

tors similarly to even-even nuclei. We then compare levels of ^{25}Mg obtained by the MCSM with those computed by exact diagonalization in Fig. 1. The full sd shell is taken, and the USD interaction [17] is used. Hereafter, J and M denote the total angular momentum and its z component, respectively. The m-scheme shell-model dimension is 44 133 for $M=1/2$. In odd-A nuclei, energies of low-lying yrast states do not necessarily become higher as J increases, and hence one has to use the J-compressed basis vectors generated with the full angular momentum projection [11]. The calculated results are shown in Fig. 1, where one finds that the MCSM results come close to the exact ones for the QMCD basis dimension ~ 40, indicating the feasibility of the MCSM.

We now move on to ^{31}Na: a key nucleus known for anomalous properties of the mass [4], and the ground-state spin and magnetic moment [18,19]. Hereafter, we use a common notation, $npnh$, to imply n-particle n-hole excitation from the sd shell to the pf shell. The ground state of ^{31}Na becomes $5/2^+$ in the $0p0h$ calculation with the USD interaction [17]. The energy levels obtained by the present MCSM calculation are compared with the experiment in Fig. 2. The ground-state spin becomes $3/2^+$ in agreement with experiment. The calculated magnetic moment of the ground state is 2.17 μ_N with the free-nucleon g factors used during the present study being consistent with the experimental

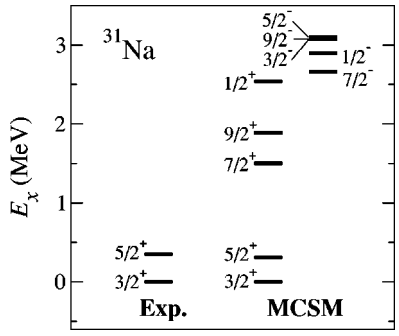

FIG. 2. Experimental energy levels of ^{31}Na (Exp.) [20] compared to those of the MCSM calculation (MCSM) for $J=1/2$ to 9/2.

value of 2.283(38) μ_N [19]. The present study shows that while the ground state is dominated by $2p2h$ excitations, $4p4h$ and higher excited configurations are mixed and they lower the ground-state energy by more than 700 keV, giving rise to a better agreement with experiment. Note that these excitations are predominantly of neutrons. The first excited state of ^{31}Na is a $5/2^+$ state at 310 keV in the present calculation. Quite recently, this state has been observed at 350 ± 20 keV [20], in excellent agreement with the calculation. This agreement supports the validity of the present Hamiltonian and model space in the study of odd-Z nuclei with $N\sim 20$. The value, $B(E2;3/2^+\rightarrow 5/2^+)=200$ e^2 fm^4, is obtained with the effective charges $e_p=1.3e$ and $e_n=0.5e$ [13] which are also adopted throughout the present study. This $B(E2)$ value corresponds to $\beta_2=0.53$ (i.e., intrinsic electric quadrupole moment $Q_0\sim 60$ e fm^2) by assuming an axially symmetric rotor with $K=3/2$, indicating a strong deformation. This β_2 value is similar to the value obtained for the adjacent even-A nucleus ^{32}Mg [21]. $E2$ properties of the ground state $B(E2;3/2^+_1\rightarrow 5/2^+_1,7/2^+_1)$ and $Q(3/2^+_1)$ are consistent with the above Q_0. The value, $B(M1;5/2^+\rightarrow 3/2^+)=0.32$ μ_N^2, is obtained. From these values the $E2/M1$ mixing ratio turns out to be 3.5×10^{-3} for the transition $5/2^+\rightarrow 3/2^+$, suggesting $M1$ dominance for this decay. The conventional shell-model calculation without mixing of different particle-hole configurations produces somewhat similar but deviating results [7,20]. For instance, the $5/2^+$ level has been predicted around 200 keV in [6,7,20], which is very similar to the result of the calculation restricted to the $0p0h+2p2h$ configurations with the present interaction.

In order to see the underlying mechanism of shell-model results, we can make use of *effective* (spherical) *single-particle energies* (ESPE's), which represent mean effects from the other nucleons on a nucleon in a single-particle orbit. The naive filling configuration is usually assumed. The two-body matrix element of the interaction depends on the angular momentum coupled by two interacting nucleons, but, in the so-called monopole Hamiltonian, this dependence is averaged out as explained in [22,13]. The ESPE is obtained from this monopole Hamiltonian, and was evaluated for $N\sim 20$ nuclei in [13] from the present Hamiltonian. The effective shell gap, the difference of ESPE's, turned out to be considerably small between the sd and pf shells for neutrons in exotic nuclei with $N\sim 20$: ~ 3 (4) MeV for ^{30}Ne (^{32}Mg), whereas it is ~ 6 MeV for ^{40}Ca [13]. A varying shell gap is discussed within HFB calculations in [23].

We next examine the two-neutron separation energies (S_{2n}). Figure 3(a) exhibits measured [24] and calculated S_{2n}, which are in agreement with each other. The mass of ^{30}Ne has been remeasured quite recently [25], showing a value closer to the calculation. For comparison, the $0p0h$ calculation is included in Fig. 3(a). The $0p0h$ results indicate considerable discrepancies from experiment for smaller Z, while the agreement is not so bad for $Z\sim 14$, implying the restoration of the $N=20$ magic structure in stable nuclei. The S_{2n} values of $2p2h$ unmixed conventional calculations in [3,7] show certain improvement (~ 1 MeV) from the $0p0h$

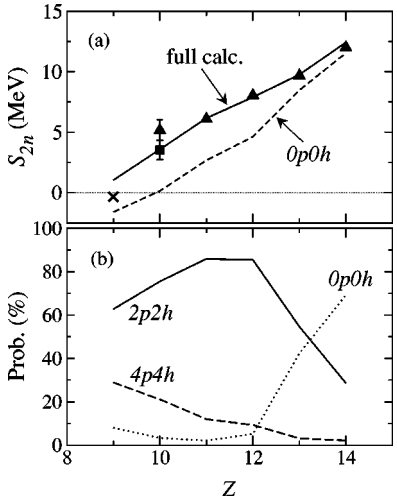

FIG. 3. (a) Two-neutron separation energies of $N=20$ isotones. Triangles denote the experimental values in [24], while the square for ^{30}Ne is a recent datum [25]. Solid and dashed lines correspond to the full and $0p0h$ calculations with the present interaction, respectively. The cross for ^{29}F means the $0p0h+2p2h$ truncation. (b) Probabilities of $0p0h$, $2p2h$, and $4p4h$ configurations in the ground state of $N=20$ isotones, indicated by dotted, solid, and dashed lines, respectively.

results, while the experimental values are still larger by another ~ 1 MeV for ^{31}Na and ^{32}Mg, for instance.

We now focus on ^{29}F, and discuss first why it is difficult to have unbound ^{26,28}O and bound ^{29}F at the same time. Unbound ^{26,28}O most likely indicate an unbound neutron $0d_{3/2}$ orbit, as is the case in the present work. This implies that, although the $0d_{3/2}$ orbit may be bound in F isotopes due to one more proton, it should not be bound too deeply. If one compares ^{27}F and ^{29}F assuming the $N=20$ magic structure, ^{27}F has two valence neutron holes, whereas ^{29}F has none. The energy gain due to valence nucleon interactions is present only for ^{27}F, and cancels and probably overcomes the gain in ^{29}F by putting two more neutrons in $0d_{3/2}$ which is only moderately deep. Thus, with the $N=20$ magic structure, it is very unlikely to have unbound ^{26,28}O and bound ^{29}F. Indeed, Fig. 3(a) indicates that ^{29}F is not bound in the $0p0h$ calculation. Note that the other isotones are bound, apart from deviations in the S_{2n} values. The result obtained by mixing the $0p0h$ and $2p2h$ configurations is also shown in Fig. 3(a). In this extended space, ^{29}F remains still unbound. This difficulty is quite general, as a similar situation can be found in [7]. On the other hand, the present calculation with full mixing produces a bound solution for ^{29}F which is consistent with the experiment [1]. In order to see the binding mechanism of ^{29}F, we now analyze the structure of the ground-state wave functions.

Figure 3(b) shows probabilities of $0p0h$, $2p2h$, and $4p4h$ configurations in the ground state of $N=20$ isotones. While the $2p2h$ configurations are dominant in ^{31}Na and ^{32}Mg, the strong mixing of $4p4h$ ones is evident in ^{29}F and ^{30}Ne. The dominance of the $2p2h$ configuration in ^{31}Na and ^{32}Mg compared to ^{29}F and ^{30}Ne is consistent with a large static quadrupole deformation which pulls down a deformed (or Nilsson-like) orbit from the pf shell below an uprising deformed orbit from the sd shell. Indeed, the yrast states of ^{31}Na are described by an axially symmetric rotor having $Q_0 \sim 60$ e fm^2 as already discussed. On the other hand, for ^{29}F a smaller intrinsic electric quadrupole moment is obtained from the shell-model quadrupole moment of the $5/2^+$ ground state as $Q_0=-36$ e fm^2 by assuming $K=5/2$.

TABLE I. Two-neutron separation energy of ^{29}F decomposed to different origins such as the bare single-particle energy (Bare SPE) and the $T=0$ and 1 two-body interactions. The second to fifth rows stand for the S_{2n} calculated by the monopole Hamiltonian and the ones obtained for the $0p0h$, $0p0h+2p2h$, and full configurations, respectively. The energies are in MeV. The last column shows the quadrupole moment of the ground state of ^{29}F in e fm^2.

	Bare SPE	$T=0$	$T=1$	Total	Q
Monopole	-3.29	$+3.28$	$+1.66$	$+1.65$	-9.0
$0p0h$	-2.70	$+1.73$	-0.63	-1.60	-9.0
$0p0h+2p2h$	-3.65	$+2.67$	$+0.61$	-0.37	-12.0
Full	-5.09	$+2.62$	$+3.50$	$+1.03$	-13.0

The large $4p4h$ probability in ^{29}F and ^{30}Ne is clearly due to the narrowing of the effective shell gap for neutrons. Owing to such particle-hole excitations, large correlation energies can be gained, and ^{29}F becomes bound in this work. In order to see this mechanism in more detail, we decompose the Hamiltonian into the bare single-particle energy and the $T=0$ and 1 two-body interactions. Table I shows their contributions to S_{2n} of ^{29}F.

We first investigate the S_{2n} of ^{29}F obtained from the monopole Hamiltonian with the filling configuration for both ^{27}F and ^{29}F. Although the $0d_{3/2}$ bare single-particle energy is positive, the total monopole effect on this S_{2n} is positive because of gains from $T=0$ and 1 two-body interactions. Note that, if the contribution of the $T=0$ part is dropped off as in the case of O isotopes, the S_{2n} becomes negative. Thus, the $T=0$ contribution to the present monopole effect is crucial, whereas the effect of the $T=1$ part is smaller. Table I also shows the quadrupole moment of the ^{29}F ground state, which is equal to the single valence proton value in this ''monopole'' calculation, because of the $N=20$ closed shell.

We now come back to the original Hamiltonian, and diagonalize it in order to see effects of dynamical correlations. In the $0p0h$ configurations, the dynamical correlations are relevant only to ^{27}F, which makes the present S_{2n} negative. Table I shows that both the $T=0$ and 1 contributions to this S_{2n} are smaller than the corresponding values with the monopole Hamiltonian.

We next extend the model space so as to include up to the $2p2h$ configurations. Both the $T=0$ and 1 contributions to the S_{2n} become larger by ~ 1 MeV. The correlation energy of ^{29}F is increased and the total S_{2n} is raised, but it still remains negative, failing to bind ^{29}F. Note that the quadrupole moment of the ground state of ^{29}F is increased by $\sim 30\%$ from the $0p0h$ calculation.

Finally, we come to the calculation with full configurations. The major change from the $0p0h+2p2h$ result is the dramatic increase of the $T=1$ contribution which is about 3

MeV. The bare single-particle energy produces a negative effect -1.4 MeV to the S_{2n}, reflecting more particle-hole excitations. The $T=0$ contribution to this change is negligible. Nevertheless, the total S_{2n} increases by ~ 1.4 MeV, and finally becomes positive. Because the major effect of the $T=1$ interaction comes from the pairing, the large $T=1$ gain means that the pairing correlation is strongly enhanced in moving from the $0p0h+2p2h$ to the full configurations. Out of the total $T=1$ contribution to the S_{2n} (3.5 MeV as shown in Table I), the cross-shell monopole pairing accounts for 1.2 MeV, while the monopole pairing within the pf shell for 1.5 MeV. Thus, these two are equally important. We now see a sharp contrast to the energy gain from the $0p0h$ to the $0p0h+2p2h$, where both the $T=0$ and 1 contribute to similar extents. The binding energy gain beyond the $2p2h$ configurations is only 0.2 MeV for ^{27}F, whereas it is 1.6 MeV for ^{29}F. Because the major origin of the deformation energy is the $T=0$ interaction, the primary source of this large energy gain of ^{29}F is not the deformation but the pairing. This point can be confirmed from the quadrupole moment shown in Table I: despite the large mixing of higher intruder configurations, ^{29}F remains only modestly deformed. Thus, by having such higher configurations beyond $2p2h$, the pairing correlations become enhanced over single-particle states of the sd and pf shells, and bring about a crucial piece of binding energy to make ^{29}F bound. On the other hand, because of lower Fermi energy, such a strong enhancement of the pairing correlations does not occur in ^{27}F.

In the O isotopes, due to no valence proton, the ESPE of the neutron $0d_{3/2}$ is higher than in the F isotopes. Moreover, the gain by dynamical correlations comes only from the $T=1$ interaction and cannot overcome this higher ESPE of $0d_{3/2}$. The drip line of O isotopes is hence determined by the completion of the occupancy of the $1s_{1/2}$ orbit, and is located closer to the β-stability line.

Since the mixing among different particle-hole configurations plays crucial roles, we should investigate cases where such mixing can be discussed. This may be done for ^{34}Si: in Fig. 3(b), the $0p0h$ configuration is mixed with the $2p2h$ rather strongly in its ground state. Figure 4 shows the 2_1^+ and 4_1^+ states of ^{34}Si, which comprise mainly $2p2h$ configurations [13], as seen well below what is expected in the shell model within the sd shell [26]. The observed small value of $B(E2;0_1^+ \rightarrow 2_1^+)$ [27] is consistent with the present structure of the 0_1^+ and 2_1^+ states. It has been reported recently that a candidate for the second (i.e., ''intruder'') 0^+ is observed at 2.13 MeV [28]. The present 0_2^+ state is at 2.07 MeV in Fig. 4, and is of $\sim 80\%$ $2p2h$. This result is compared, in Fig. 4, to other shell-model calculations predicting similar structures. In the calculation by Caurier *et al.* [7], the lowest pure $2p2h$ 0^+ eigenstate is located at 1.7 MeV above the pure $0p0h$ 0^+ ground state. After the mixing between them, the excitation energy rises to 3.0 MeV. The calculation by Baumann *et al.* [26] has adopted a more restricted space, resulting in higher excitation energy. Higher intruder configurations should lower this level.

In other shell-model calculations including the *island of inversion* picture [3,7], ^{33}Al is classified as a normal nucleus,

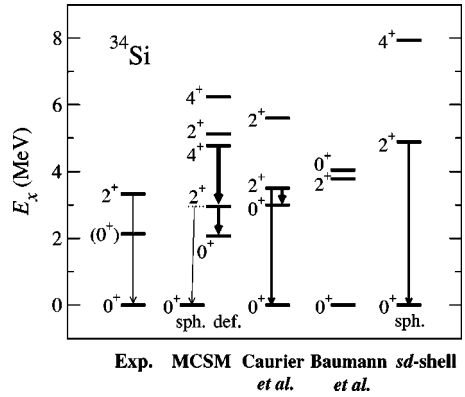

FIG. 4. Experimental energy levels of ^{34}Si (Exp.) compared with those of shell model calculations by the present study (MCSM), Caurier *et al.* [7], Baumann *et al.* [26], and the sd-shell model with the USD [17]. The width of the arrows illustrates the $B(E2)$ value, while no $B(E2)$ values are reported in [26].

while a substantial mixing of intruder configurations occurs in this work as shown in Fig. 3(b). The magnetic dipole and electric quadrupole moments of the $5/2^+$ ground state are, in the present calculation, 3.88 μ_N and 16.0 e fm, respectively, while they are 4.25 μ_N and 11.8 e fm in the sd-shell model with the USD. The intruder configurations are more important for some low-lying states: in the sd-shell picture, the $1/2_1^+$ level is at 3.1 MeV, and its wave function is dominated by a proton $(0d_{5/2})^4(1s_{1/2})^1$ configuration because of the stiff proton $(0d_{5/2})^n$ core. This level comes down to 1.3 MeV, once intruder configurations are included. The state is then dominated by $2p2h$ configurations, and the stiff proton core is destroyed substantially.

As suggested in [29] and confirmed later, for instance, in [30], the closed shell is broken significantly in ^{16}O. It is then of great interest to compare the present case to ^{16}O. Apart from apparent similarities, there are three major differences: (i) a proton and a neutron are excited together in ^{16}O to a large extent, whereas basically only neutrons are excited in the present case, because only the neutron gap becomes narrow and only the neutron Fermi energy is high, (ii) the shell gap is large in ^{16}O, whereas it varies in the $N=20$ isotones and the present issue is strongly linked to nuclei with smallest gaps, (iii) in some nuclei in the present case the ground state is predominantly comprised of intruder configurations, while the closed shell remains a major configuration ($\sim 40\%$) of the ground state of ^{16}O [30].

In conclusion, we presented a systematic study for $N=20$ isotones, which gives rise to the drip line of F isotopes located extremely far. The feasibility of the odd-A MCSM calculation is confirmed. The properties of ^{31}Na are reproduced in good agreement with the experiment, indicating the validity of the present Hamiltonian and model space for odd-Z nuclei with $N=20$. ^{29}F is bound. While it has been rather difficult to obtain unbound ^{26,28}O and bound ^{29}F, a solution appeared naturally in the present work in a general framework for stable and exotic nuclei. Although the ground states primarily comprise the $2p2h$ configurations in nuclei such as ^{31}Na and ^{32}Mg consistently with the *island of inversion* model, the mixing of $4p4h$ and higher intruder states is en-

hanced by the narrowing of the shell gap in some other nuclei. The binding of ^{29}F is an example of such mixing, while it is not the case even with the present Hamiltonian if the configurations are restricted up to $2p2h$. This seems to be a new mechanism of extending the drip line and should be explored further. ^{31}F is still unbound in the present work; we probably have to include effects of neutron halo. In fact, by lowering the neutron $1p_{3/2}$ by 350 keV, both ^{29}F and ^{31}F become bound. This amount of lowering is quite possibly a consequence of a halo(like) structure. We finally comment that the MCSM has made it possible to carry out full mixing of particle-hole configurations and has played a crucial role in this work.

We acknowledge Professor A. Gelberg for reading the manuscript. The MCSM calculations were performed by the Alphleet computer in RIKEN. The conventional shell-model calculations were made by the codes OXBASH [31] and MSHELL [32]. This work was supported in part by Grant-in-Aid for Scientific Research No. (A)(2) (10304019) from the Ministry of Education, Science and Culture.

[1] D. Guillemaud-Mueller *et al.*, Z. Phys. A **332**, 189 (1989).
[2] H. Sakurai *et al.*, Phys. Lett. B **448**, 180 (1999), and references therein.
[3] E.K. Warburton, J.A. Becker, and B.A. Brown, Phys. Rev. C **41**, 1147 (1990).
[4] C. Thibault *et al.*, Phys. Rev. C **12**, 644 (1975).
[5] A. Poves and J. Retamosa, Phys. Lett. B **184**, 311 (1987); Nucl. Phys. **A571**, 221 (1994).
[6] N. Fukunishi, T. Otsuka, and T. Sebe, Phys. Lett. B **296**, 279 (1992).
[7] E. Caurier, F. Nowacki, A. Poves, and J. Retamosa, Phys. Rev. C **58**, 2033 (1998).
[8] M. Honma, T. Mizusaki, and T. Otsuka, Phys. Rev. Lett. **75**, 1284 (1995).
[9] T. Mizusaki, M. Honma, and T. Otsuka, Phys. Rev. C **53**, 2786 (1996).
[10] M. Honma, T. Mizusaki, and T. Otsuka, Phys. Rev. Lett. **77**, 3315 (1996).
[11] T. Otsuka, M. Honma, and T. Mizusaki, Phys. Rev. Lett. **81**, 1588 (1998).
[12] T. Otsuka, T. Mizusaki, and M. Honma, J. Phys. G **25**, 699 (1999).
[13] Y. Utsuno, T. Otsuka, T. Mizusaki, and M. Honma, Phys. Rev. C **60**, 054315 (1999).
[14] A. Azaiez *et al.*, in *Nuclear Structure 98*, edited by C. Baktash, AIP Conf. Proc. No. 481 (AIP, Woodbury, New York, 1999), p. 243.
[15] B.V. Pritychenko *et al.*, Phys. Lett. B **461**, 322 (1999).
[16] P.B. Radha *et al.*, Phys. Rev. C **56**, 3079 (1997); D. J. Dean (private communication).
[17] B.A. Brown and B.H. Wildenthal, Annu. Rev. Nucl. Part. Sci. **38**, 29 (1988).
[18] X. Campi *et al.*, Nucl. Phys. **A251**, 193 (1975).
[19] G. Huber *et al.*, Phys. Rev. C **18**, 2342 (1978).
[20] B.V. Pritychenko *et al.*, Phys. Rev. C **63**, 011305(R) (2001).
[21] T. Motobayashi *et al.*, Phys. Lett. B **346**, 9 (1995).
[22] A. Poves and A. Zuker, Phys. Rep. **70**, 235 (1981).
[23] P.-G. Reinhard *et al.*, Phys. Rev. C **60**, 014316 (1999).
[24] G. Audi *et al.*, Nucl. Phys. **A624**, 1 (1997).
[25] F. Sarazin *et al.*, Phys. Rev. Lett. **84**, 5062 (2000).
[26] P. Baumann *et al.*, Phys. Lett. B **228**, 458 (1989).
[27] R.W. Ibbotson *et al.*, Phys. Rev. Lett. **80**, 2081 (1998).
[28] S. Nummela *et al.*, Phys. Rev. C **63**, 044316 (2001).
[29] G.E. Brown and A.M. Green, Nucl. Phys. **75**, 401 (1966).
[30] W.C. Haxton and C. Johnson, Phys. Rev. Lett. **65**, 1325 (1990).
[31] A. Etchegoyen *et al.*, MSU-NSCL Report No. 524, 1985.
[32] T. Mizusaki, RIKEN Accel. Prog. Rep. **33**, 14 (2000).